Differential scanning calorimetry of polymer glasses: corrections for thermal lag

J. M. Hutchinson, M. Ruddy and M. R. Wilson
Department of Engineering, Aberdeen University, Aberdeen AB9 2UE, UK
(Received 21 April 1987; revised 23 June 1987; accepted 4 August 1987)

A theoretical treatment of the kinetics of structural recovery of polymer glasses is applied to 'intrinsic' thermal cycles. These cycles involve cooling a sample at constant rate q_1 from an equilibrium state at high temperature through the glass transition region to a lower temperature T_1, and then immediately reheating the sample at constant rate q_2. In differential scanning calorimetry (d.s.c.), a peak in the specific heat capacity is observed during the heating stage, occurring at a temperature T_p which depends upon both the cooling and the heating rates. For a fixed ratio of these rates, such intrinsic cycles yield heating isobars of identical shape, but shifted along the temperature scale by an amount which depends upon the heating (or cooling) rate. The invariance of the peak shape, and in particular the peak width, is shown to provide a means of correcting d.s.c. data for thermal lag on heating. Experimental data for a low molecular weight polystyrene, when corrected for thermal lag in this way, are shown to agree with the predictions of the kinetic model for structural recovery. An analytical treatment of heat transfer in the d.s.c. cell is also described, and the theoretical results are compared with the experimental data.

(Keywords: structural recovery; polymer glasses; differential scanning calorimetry; thermal lag)

INTRODUCTION

Differential scanning calorimetry (d.s.c.) is a widely used technique for the study of thermal events in polymers and other materials. In particular, the application of d.s.c. to the glass transition region of amorphous polymers has received considerable attention over many years in attempts to characterize and to model the structural recovery of polymer and other glasses (see, for example, references 1–7). The usual procedure here is first to cool the sample, at a constant rate, then to anneal it for a fixed period at a temperature below the glass transition temperature T_g, and finally to heat it at a constant rate through the transition region. The d.s.c. output is proportional to the specific heat C_p of the sample, which typically passes through a maximum on heating, going from a value characteristic of the glass, C_{pg}, to one characteristic of the liquid, C_{pl}. The position of this maximum on the temperature scale and its height are both dependent on the whole previous thermal history of the sample[1–8], and in particular on the amount of annealing at the lower temperature and on the heating rate. Such effects are clearly shown qualitatively by d.s.c., but an analysis of structural recovery requires a quantitative interpretation of the data. This latter is hindered by the problem of experimental thermal lag, which has the general effect of broadening the sample response; the degree of broadening is dependent on the heating rate, and it is particularly evident for the faster heating rates.

It is not always clear in the literature whether or not published data have been corrected for thermal lag; furthermore, in some instances where corrections have been made, it is not obvious just how the relevant corrections have been applied. Nevertheless, it is accepted[9] that significant thermal gradients exist in d.s.c., and methods of correcting for thermal lag have been suggested[10,11]. These corrections involve contributions to the thermal lag which originate either in the instrument itself or in the sample material. The former corrections are easier to make and involve a calibration of the temperature scale by reference to a fixed temperature, typically the melting temperature of a pure metal such as indium. Since finite heating rates cause the melting endotherm to be less than perfectly sharp, the usual procedure[11] is to define a 'dynamic' melting temperature as the temperature of intersection of the extrapolated leading edge of the melting endotherm with the extrapolated baseline.

The latter corrections, i.e. those that result from thermal lag within the sample material itself, are, however, harder to make. Procedures involving the use of different sample masses have been suggested[9], with an extrapolation to zero mass defining the thermal lag. This, however, has some problems: for example, only a limited range of sample masses is available for which adequate sensitivity from the instrument can be maintained.

The present paper suggests an alternative procedure for correcting for thermal lag during heating. It is based upon the results of a theoretical treatment of structural recovery in the glass transition region originally developed by Kovacs, Aklonis, Hutchinson and Ramos, now commonly known as the KAHR model[12]. This model predicts a response to certain three-step thermal cycles in which no thermal lag occurs; experimental data are compared with this theoretical model, and the resulting thermal lag is analysed and then discussed in terms of the temperature gradients existing within the system during the heating stage of these cycles.

THEORY

The isobaric response of glasses to any prescribed thermal treatment can be obtained by an analysis based

0032-3861/88/010152-08$03.00

on the KAHR model[12]. Of particular interest in most studies of the kinetics of structural recovery is the thermal treatment involving a three-step cycle. Here the sample is cooled at a constant rate q_1 (K min^{-1}) from equilibrium at a temperature T_0 ($\gg T_g(q_1)$) to a temperature T_1 below $T_g(q_1)$, where $T_g(q_1)$ is the glass transition temperature relevant to the cooling rate q_1. The sample may then be annealed at T_1 before reheating at a constant rate q_2 (K min^{-1}) until equilibrium is again established. Within this general scheme of three-step thermal cycles is the particular variant known as the 'intrinsic' cycle, for which the sample is not annealed at T_1 (i.e. annealing time is zero) before reheating; such intrinsic thermal cycles are therefore defined by only three experimental variables: q_1, q_2 and T_1. It can be shown[12-14] that, on heating, the thermal expansion coefficient or the specific heat capacity C_p passes through a maximum at a temperature T_p which depends upon these experimental variables. The dependence of T_p on each experimental variable in turn is defined through the partial derivatives:

$$s(T_1)=\left(\frac{\partial T_p}{\partial T_1}\right)_{q_1,q_2} \quad (1)$$

$$s(q_1)=\left(\frac{\partial T_p}{\partial \ln|q_1|}\right)_{T_1,q_2} \quad (2)$$

$$s(q_2)=\left(\frac{\partial T_2}{\partial \ln q_2}\right)_{T_1,q_1} \quad (3)$$

Note that each derivative is evaluated with the other two variables held constant. Furthermore, one can show[12-14] that, for $T_1 \ll T_g(q_1)$, $s(T_1)$ in such cycles is indistinguishable from zero; in other words, the temperature T_p is independent of the lower temperature T_1 of the thermal cycle provided that the cooling stage proceeds to a sufficiently low temperature. This important observation will be referred to again later in this section.

The peak temperature T_p is therefore dependent only on the cooling and heating rates, q_1 and q_2, respectively, used in these cycles. These dependencies have been evaluated theoretically from numerous cycles involving various combinations of q_1 and q_2; this has been done for systems based upon both the discontinuous KAHR multiparameter model[12] and a continuous spectrum[15] in which the recovery function is described by a 'stretched exponential' empirical expression now known as the Williams–Watts function[16]. Both treatments give identical results in respect of the partial derivatives defined in equations (1)–(3). Of particular interest here is a special case of these intrinsic cycles, in which the ratio of cooling rate to heating rate, $R=|q_1|/q_2$, is held constant. The heating stages of three such cycles are illustrated in *Figure 1*, for which a ratio $R=1$ has been used. These theoretical curves were generated using the Williams–Watts function with parameter values indicated in the caption.

It is clear from *Figure 1* that the heating stages of intrinsic cycles, for which the same ratio R pertains, result in peaks in the specific heat capacity or thermal expansion coefficient which are exactly superposable by a shift along the temperature scale. This shift can, in fact, be shown to be related to the partial derivatives defined in equations (2) and (3):

$$\frac{dT_p}{d\ln|q_1|}=\frac{dT_p}{d\ln q_2}=s(q_1)+s(q_2)=\theta^{-1} \quad (4)$$

where θ is a material parameter characterizing the temperature dependence of the retardation times in equilibrium[12]. The importance of this exact superposition of the peaks in the present context is that the peak shape, or, more precisely, the peak width which will be used later, is an *invariant* under these experimental conditions. That is, the widths of C_p or α peaks on heating at a rate q_2 *immediately* (no annealing) after cooling from equilibrium above T_g at a rate q_1 are theoretically constant for intrinsic cycles in which the ratio $R=|q_1|/q_2$ is fixed. Any experimentally observed deviation from a constant peak width must therefore reflect a broadening resulting from thermal lag, and this provides a means of making quantitative corrections in a manner to be described below.

An important aspect of this procedure concerns the thermal lag in the sample that will inevitably be present during the *cooling* stage. Here the sample temperature will be greater than the set heater temperature by an amount which depends on the cooling rate. It follows that the lower temperature $T_1+\Delta T$ experienced by the sample will be different for different cooling rates even though the instrument is programmed to stop cooling and to start heating again at a fixed temperature T_1. However, as was shown above, the peak temperature T_p is *independent* of the lower temperature T_1 (provided that T_1 is sufficiently low within the glassy region), and hence it does not matter that the sample lower temperature exceeds the set heater temperature by a small temperature difference ΔT.

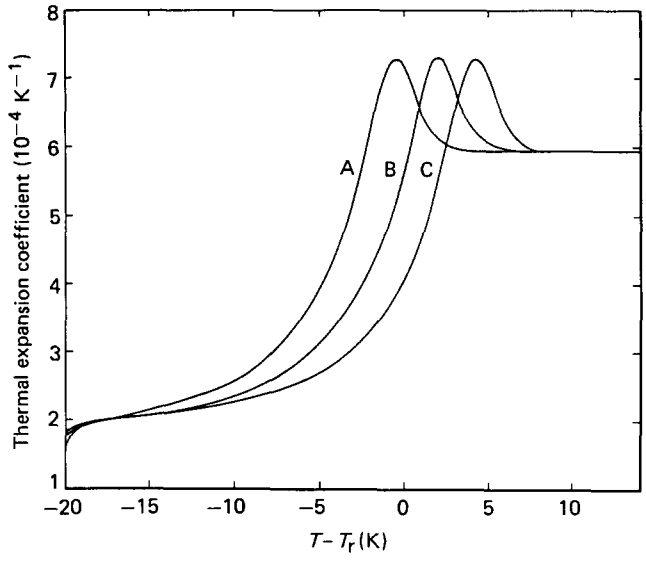

Figure 1 Theoretical heating isobars of thermal expansion coefficient as a function of $T-T_r$, where T_r is a reference temperature. The Williams–Watts function was used with sub-exponential parameter $\beta=0.456$, and the other material parameter values were: $\Delta\alpha=4.0\times10^{-4}$ K^{-1}, $\alpha_l=6.0\times10^{-4}$ K^{-1}, $\theta=1.0$ K^{-1}, $x=0.2$, $\tau_{ref}=8.32$ t.u., $T_0-T_r=10$ K, $T_1-T_r=-20$ K, $\Delta\delta=0$ (for nomenclature see refs. 12–15). Values of q_1 and q_2 (in units of K t.u.$^{-1}$) are as follows, the ratio being $R=1$ in all cases: curve A, $q_1=-0.01$, $q_2=+0.01$; curve B, $q_1=-0.1$, $q_2=+0.1$; curve C, $q_1=-1.0$, $q_2=+1.0$

Table 1 Combination of cooling and heating rates to achieve the given values of R

q_2 (K min^{-1})	q_1 (K min^{-1}) for $R=0.33$	$R=0.5$	$R=1.0$
2.5	0.8	1.3	2.5
5.0	1.7	2.5	5.0
7.5	2.5	3.8	7.5
10.0	3.3	5.0	10.0
12.5	4.1	6.3	12.5
15.0	5.0	7.5	15.0
17.5	5.8	8.8	17.5
20.0	6.7	10.0	20.0
25.0	8.3	12.5	–
30.0	10.0	15.0	–
35.0	11.7	17.5	–
40.0	13.3	20.0	–

Equation (4) above shows also that the material parameter θ can be evaluated by determining experimentally the dependence of the peak temperatures T_p, in such intrinsic cycles with fixed R, on the cooling or heating rates. Furthermore, since θ is a constant, a linear dependence of T_p on $\ln|q_1|$ or $\ln q_2$ should be observed.

EXPERIMENTAL

A narrow fraction atactic polystyrene ($\bar{M}_w/\bar{M}_n < 1.1$) with a molecular weight of 2820 from Polymer Laboratories Ltd was used in this study. A single sample of mass 20.02 mg was used throughout. This polystyrene has a dilatometric glass transition temperature in the region of 71°C.

The polystyrene sample was subjected to all thermal cycles within the cell of a Perkin–Elmer DSC-4 differential scanning calorimeter. These thermal cycles involved heating the sample to a temperature of 120°C and equilibrating for 5 min; cooling at a constant rate q_1 to a lower temperature T_1, which was either 55°C or 40°C in two series of experiments performed; and, finally, reheating immediately at a constant rate q_2 until equilibrium is again established at 120°C. Controlled cooling rates between 0.8 K min^{-1} and 20 K min^{-1} were used, the upper limit being the maximum cooling rate that could be achieved with the normal head with cooling water flowing. Heating rates between 2.5 K min^{-1} and 40 K min^{-1} were used, with values chosen such that a number of cycles with different ratios R could be achieved. The combinations of cooling and heating rates are given in *Table 1*.

At each heating rate the temperature scale calibration was carried out as described elsewhere[11], using indium as the calibrant. Immediately after this, and before performing any experiments, the baseline was optimized over the whole experimental temperature range and for 10 K beyond the upper (T_0) and lower (T_1) temperatures. The instrument sensitivity was set at maximum and the encapsulated sample was placed centrally in the cell, as was the empty reference pan. Care was taken to ensure that neither the sample nor the reference pan moved on closing the cover of the d.s.c. cell.

For each heating rate, a series of experiments was performed involving the cooling rates listed in *Table 1*. Throughout this series of experiments, the sample remained in the d.s.c. cell. This procedure removed any experimental error which could have arisen if the sample location within the cell had been altered between each experiment.

The heating stages of these intrinsic cycles gave rise to peaks in the differential power output from the d.s.c., in the usual way. The characteristic features of these peaks of particular importance here are the peak temperature T_p and the peak width W. These are illustrated in *Figure 2*, the peak width being determined as follows. An inflexional tangent was drawn to the rise of the peak, and its intersection with the extrapolated glassy baseline defined an initial onset temperature T_i. Similarly, the inflexional tangent to the fall of the peak intersected the extrapolated liquid baseline at a final temperature T_f. The width W of the peak is defined as the difference, $T_f - T_i$, between the final and initial peak temperatures.

RESULTS

Figure 3 shows the heating stage of three intrinsic cycles for which the cooling rate was half the heating rate ($R=0.5$) and involving a lower temperature T_1 of 40°C. Theoretically, in the absence of thermal lag, each peak should be identical in shape but displaced along the temperature axis. Clearly this is not the case: the peak broadens as the heating rate increases. Consider also the

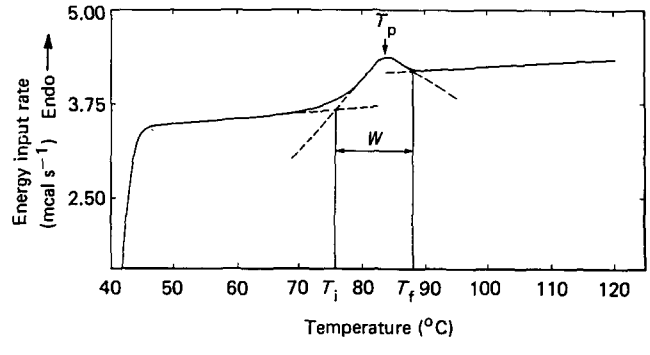

Figure 2 Typical experimental heating isobar (energy input rate versus temperature) for an intrinsic thermal cycle. The peak width W is defined by the use of inflextional tangents intersecting, at T_i and T_f respectively, the extrapolations of the asymptotic glassy region and the equilibrium liquid. The temperature T_p is the temperature at which the maximum in the peak occurs

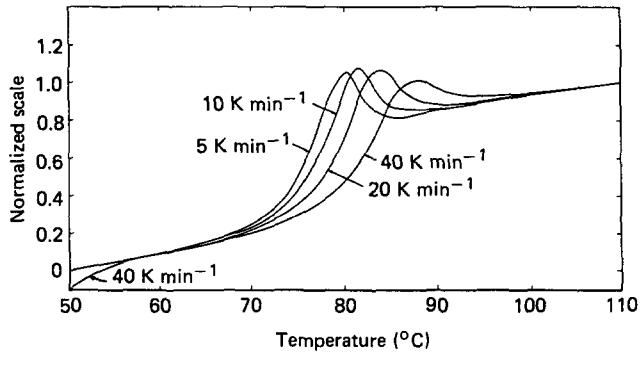

Figure 3 Experimental heating isobars for intrinsic thermal cycles with $R=0.5$, and with the particular values of heating rate indicated. The ordinate is the normalized power output from the d.s.c., on a scale from zero at 50°C to unity at 110°C. The cycles involved had $T_0=120$°C and $T_1=40$°C, though only part of this temperature range is shown in the figure. Note the departure of the curve for $q_2=40$ K min^{-1} from those for lower values of q_2 in the temperature range below 60°C

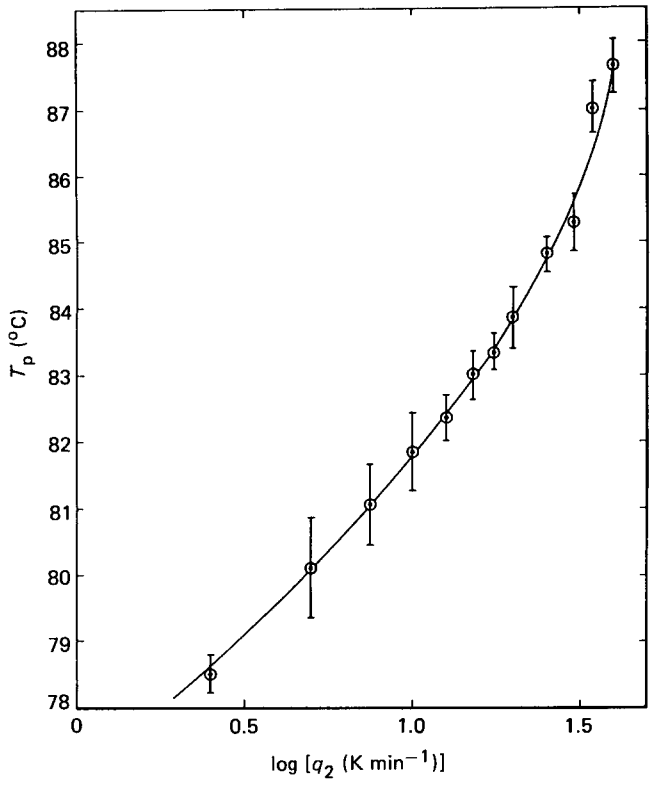

Figure 4 Variation of peak temperature T_p with log (heating rate) for intrinsic cycles with $R=0.5$ and $T_1=40°C$. The peaks in these thermal cycles were broad, with the peak temperature actually covering a range 0.5–1.5 K depending upon the heating rate. The points plotted here are the mid-points of these peak temperature ranges, and the error bars indicate the full range over which the peak temperature occurs

dependence of the peak temperatures T_p on log (heating rate), which is theoretically predicted to be linear (equation (4)). This dependence is shown in *Figure 4* for the series of intrinsic cycles for which four of the heating curves were shown in *Figure 3*. It is clear that the relationship is not linear over this range of heating rates, as is required by equation (4) for a constant value of θ. The implication of these results is that not only is the peak broadening as q_2 increases, but also the peak temperature is simultaneously being shifted to increasingly excessive values.

These discrepancies between theory and experiment result from thermal lag, and the data must be corrected to allow for this. Accordingly, the width of each peak was determined in the manner outlined in the previous section and plotted as a function of the heating rate. This procedure was adopted for each of the two series of cycles investigated here, involving lower temperatures T_1 of 55°C and 40°C. The results for each of these series are shown in *Figures 5* and *6*. These figures show that the peak width is a strong function of the heating rate, particularly at the fastest heating rates, and furthermore that the variation is the same for each value of R, the curves simply being shifted to larger peak widths as R increases.

Since the peaks in all of the heating curves used to obtain the data in each of *Figures 5* and *6* should theoretically, in the absence of thermal lag, be of the same shape, and hence of the same width, a method of correcting for this thermal lag is immediately suggested: the temperature scale within each peak should be adjusted in such a way that for each heating rate the peak width is the same. Ideally each peak should be corrected by comparison with the width of a peak for which there is no thermal lag. However, even at the slowest heating rates used here there remains evidence of significant thermal lag since the peak width still varies in this region (see *Figures 5* and *6*). Hence, it is necessary to correct the peak widths by comparison with a reference peak, which is arbitrarily chosen here to be that obtained for a heating rate of 10 K min^{-1}. The peak widths corrected in this way will not be correct in an absolute sense, but will be correct

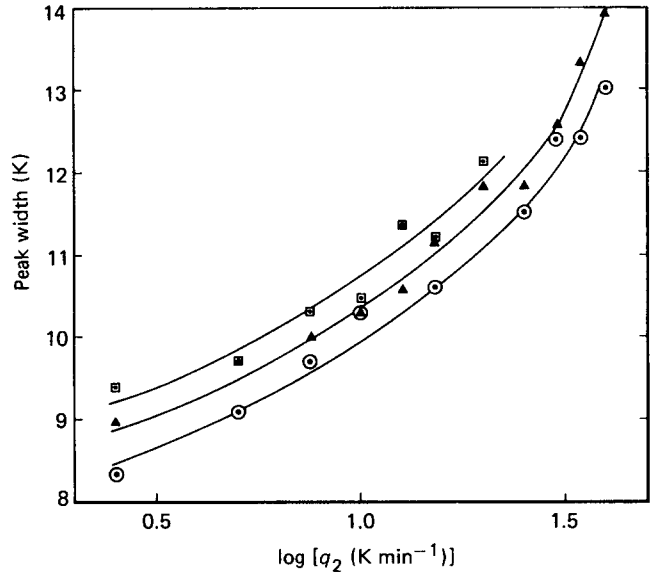

Figure 5 Peak width as a function of log (heating rate) for intrinsic cycles with $T_1=55°C$ and (⊙) $R=0.33$, (▲) $R=0.5$, (□) $R=1.0$

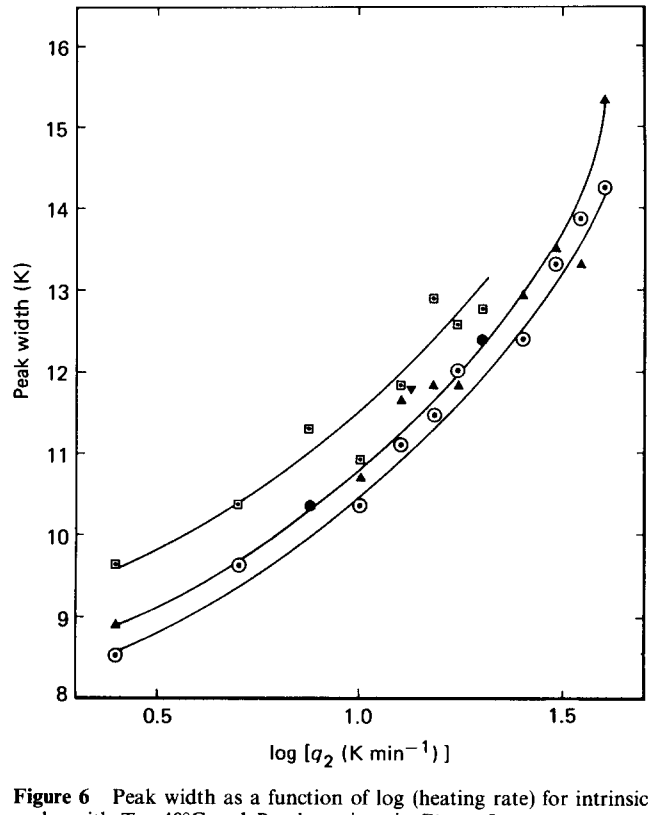

Figure 6 Peak width as a function of log (heating rate) for intrinsic cycles with $T_1=40°C$ and R values given in *Figure 5*

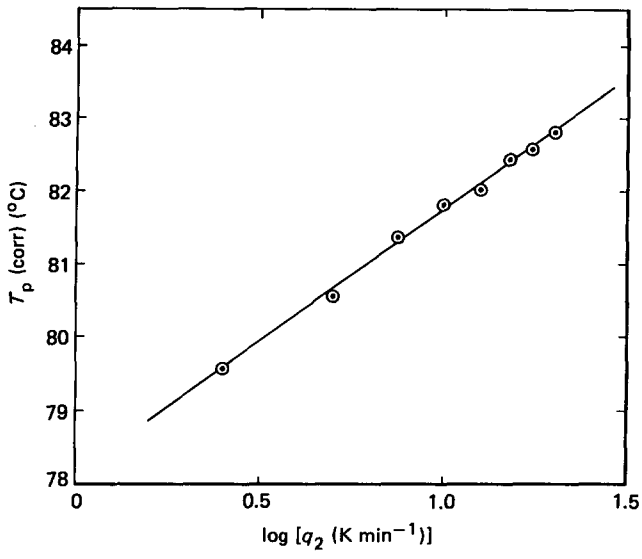

Figure 7 Variation of corrected peak temperature T_p(corr) with log (heating rate) for intrinsic cycles with $T_i = 40°C$ and $R = 0.5$

Table 2 Values of θ obtained for various ratios R and lower temperatures T_i

	θ for		
T_i (°C)	$R = 0.33$	$R = 0.5$	$R = 1.0$
55	0.48	0.55	0.70
40	0.66	0.64	0.72

relative to each other, which is all that is necessary for the present purposes.

The peak temperatures T_p are corrected as follows (refer to *Figure 2*). Theoretically, each peak for the same value of R should be of the same width W. Accordingly, to correct for thermal lag a scaling factor F_{q_2} must be applied for each heating rate q_2:

$$F_{q_2} = \frac{W_{10}}{W_{q_2}} \tag{5}$$

where W_{10} and W_{q_2} are the peak widths at the reference heating rate of 10 K min^{-1} and at q_2, respectively.

The onset temperature T_{i,q_2} is calibrated for each heating rate by reference to the melting temperature of indium. For heating rate q_2, the corrected peak temperature, T_{p,q_2}(corr), is therefore obtained by applying the scaling factor in equation (5) to the temperature difference $T_{p,q_2} - T_{i,q_2}$. Thus:

$$T_{p,q_2}(\text{corr}) = T_{i,q_2} + F_{q_2}(T_{p,q_2} - T_{i,q_2}) \tag{6}$$

The corrected peak temperatures are shown as a function of log (heating rate) in *Figure 7* for intrinsic cycles with $T_i = 40°C$. For clarity, only data corresponding to $R = 0.5$ are shown.

The curve of *Figure 4* is typical of the variation of the uncorrected peak temperatures with log (heating rate); in *Figure 7* it can clearly be seen to have been linearized by the application of the above corrections for thermal lag. The linear relationship thus obtained corresponds to equation (4) and the value of θ may be obtained directly from its slope. Values of θ have been determined in this way for each value of R and for both lower temperatures T_i of 55°C and 40°C. The results are given in *Table 2*.

THEORETICAL MODEL OF HEAT TRANSFER IN D.S.C.

When a polymer glass is heated through the transition region, the power output from the d.s.c. is observed to pass through a peak. The purpose of the heat transfer model was to show how the shape of this peak was altered as the heating rate was increased. Accordingly, a typical variation of specific heat capacity C_p with temperature was adopted as a reference and was used together with typical values for other relevant material constants to define the parameters of the model. In fact, for the purposes of this model, rather than C_p it is more convenient to use the thermal diffusivity α ($=k/\rho C_p$, where k = thermal conductivity and ρ = density); the temperature variations of both C_p and α are shown in *Figure 8*.

The thermal model is of network type, one-dimensional

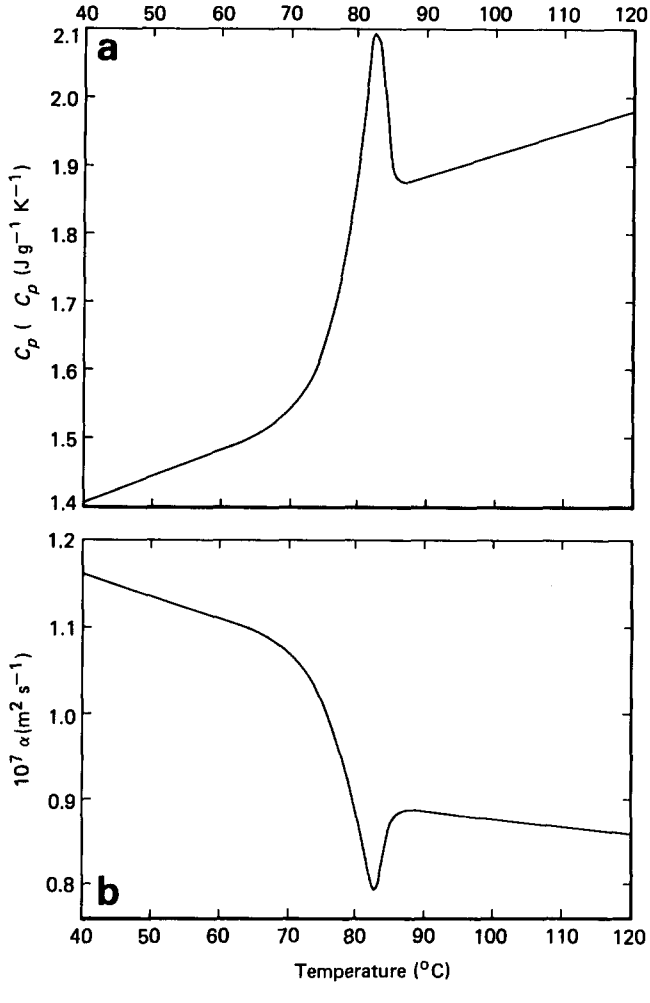

Figure 8 (a) Typical dependence upon temperature of the specific heat capacity C_p of polystyrene within the transition region. These data are used as a reference in the theoretical heat transfer model to determine the effect of sample thermal lag on peak shape. (b) The corresponding dependence upon temperature of the thermal diffusivity α of polystyrene. A typical variation of density ρ with temperature was assumed in converting from C_p to α, and a constant value of thermal conductivity $k = 0.17$ W m^{-1} K^{-1} was used

Table 3 Data relating to thermal network model

	Heating rate (K min^{-1})						
	40	20	10	5	2.5	1.2	0.5
Surface resistance, $R_s = 2.75\ 10^{-4}$ m^2 K W^{-1} (ref. 18)							
Accuracy parameter	1	1	1	1	0.5	0.5	0.25
Number of nodes	3	3	3	2	2	2	2
Time step (s)	0.219	0.219	0.219	0.465	0.931	0.931	2.327
ΔT_{01} (K)	1.015	0.521	0.264	0.181	0.090	0.043	0.018
ΔT_{1N} (K)	1.501	0.759	0.384	0.145	0.072	0.035	0.015
Peak width (K)	13.79	10.97	9.43	8.89	8.77	8.73	8.69
Surface resistance, $R_s = 5.5\ 10^{-4}$ m^2 K W^{-1}							
Time step (s)	0.251		0.251				2.592
ΔT_{01} (K)	2.530		0.336				0.022
ΔT_{1N} (K)	2.890		0.384				0.015
Peak width (K)	19.79		9.59				8.71
With aluminium pan							
Time step (s)			0.179				
ΔT_{01} (K)			0.083				
ΔT_{1N} (K)			0.384				
Peak width (K)			9.48				

ΔT_{01} = maximum value of temperature lag between set point and first node
ΔT_{1N} = maximum value of temperature lag between first and last nodes
Sample thickness = 0.75 mm
Thermal diffusivity, α – See *Figure 8*
Thermal conductivity, $k = 0.17$ W m^{-1} K^{-1}

and non-steady. Thermal capacity of the material is lumped at nodes which lie at the centres of sections of equal thickness. Thermal capacity per unit area normal to heat flow is thus given by:

$$\text{capacity} = \rho C_p t = \rho C_p t\left(\frac{k}{\alpha \rho C_p}\right) = \frac{kt}{\alpha} \qquad (7)$$

where t is the section thickness. This capacity is continuously varied as a function of node temperature according to *Figure 8*.

Thermal conductance between material nodes is simply evaluated as the ratio k/t.

The network is directly analogous to an electrical resistance/capacitance circuit. The heater 'set' temperature communicates with the nearest material node through an appropriate surface contact resistance and it is the rate of change of this set temperature with time which is the principal input parameter.

The time-step length is chosen to give an 'accuracy parameter' AP of unity. At the slowest heating rates, however, a problem arose in regard to the small size of the temperature differences between nodes, and it was necessary to reduce AP progressively to 0.25 and the number of nodes from three to two. Preston *et al.*[17], who describe the network analysis, say that values of AP down to 0.1 are normally acceptable.

Surface contact resistance is regarded as the most uncertain input parameter. A value from Fried[18] was chosen for the main series of calculations but this was arbitrarily doubled to give the second set of results in *Table 3*. Sensitivity to AP and to the number of nodes was found to be satisfactory by an unreported series of calculations. Thermal conductivity was also adjusted but found to have no outstanding effect on results. It should be noted that the aluminium sample pan was normally omitted from the model, but *Table 3* shows a single set of calculations for which this pan was included. These results are not significantly different from those obtained without inclusion of the aluminium pan, which was fortunate since the small capacity of the aluminium gave AP values which prevented evaluation at the lower heating rates. By a further small approximation, the uppermost surface was taken to be adiabatic.

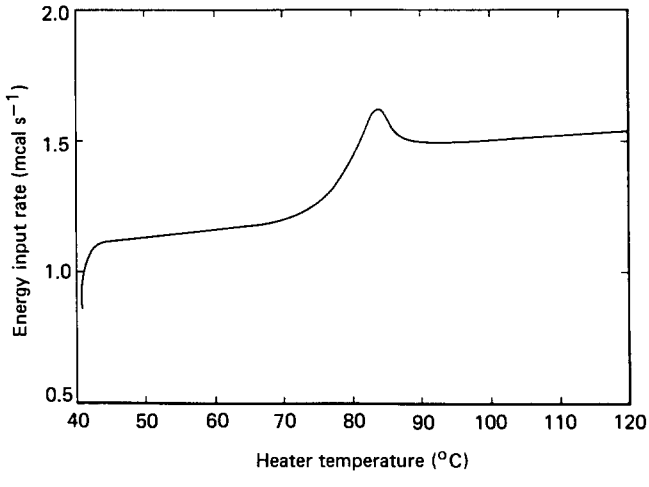

Figure 9 Typical theoretically calculated output from the d.s.c., based upon the reference C_p variation shown in *Figure 8a*. The heating rate here is 10 K min^{-1}

A typical result is shown in *Figure 9* where the energy input rate to the d.s.c. is plotted as a function of the heater temperature for a heating rate of 10 K min^{-1}. The peak width is determined for each heating rate in the manner shown in *Figure 2*, but using a routine within the computer program; the theoretical values obtained are listed in *Table 3* and plotted as a function of heating rate in *Figure 10*, together with the range of values for peak width determined experimentally.

DISCUSSION

The results presented above show how data obtained on heating a polymer glass in the d.s.c. can be corrected for

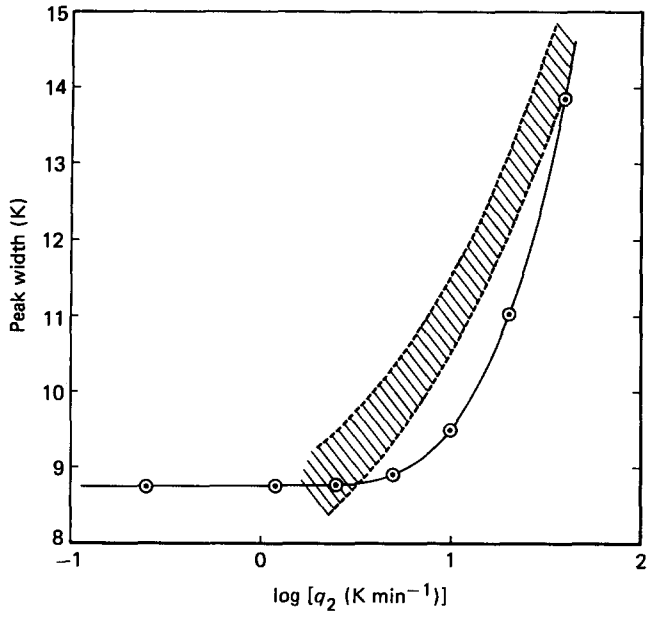

Figure 10 Variation of theoretical peak width as a function of heating rate, indicated by full line through the open circles. The shaded area gives the experimental variations for $T_1 = 40°C$, taken from *Figure 6*, over the whole range of values for R. The lower dashed line of the shaded area corresponds to $R = 0.33$, and the upper dashed line corresponds to $R = 1.0$

thermal lag. The method of correction is based on the theoretical invariance of the peak width during the heating stage of intrinsic cycles. The results in *Figure 7* show a linear dependence of the corrected peak temperature, T_p(corr), on log (heating rate), in agreement with theory (equation (4)), and with a constant value for slope from which the material parameter θ is obtained (*Table 2*).

The method of correction defined by equations (5) and (6) can be used to correct any heating scan through the glass transition region. It suffices to determine, from the appropriate intrinsic thermal cycles in the manner outlined above, the scaling factor F_{q_2} for the required heating rate q_2 relative to a reference heating rate. This scaling factor then applies to any heating scan on the same sample at the same heating rate q_2.

While this procedure appears straightforward, it is important to emphasize the need to establish a truly glassy state at the lower temperature T_1. Some of the experimental difficulties associated with this are discussed in the following sub-sections, before comparing the experimental results with the prediction of the theoretical heat transfer model.

Effect of lower temperature T_1

The parameter θ is introduced into the theory as a material constant, independent of cooling and heating rates and of the lower temperature of thermal cycles. It is, however, evident from *Table 2* that the observed value of θ for $T_1 = 55°C$ is not independent of R. These results were the first to be obtained in this work; though now known to be invalid, they have deliberately been included with the purpose of showing the dangers of using a lower temperature T_1 which is too close to the transition region.

It was shown above in the 'Theory' section that an advantage of the correction procedure employed here is that it is independent of the choice of lower temperature T_1, provided that this temperature is within the asymptotic glassy region. The temperature T_1 of 55°C was originally considered to be satisfactory since it was apparently some 16°C below the dilatometric glass transition temperature. However, two important aspects combined to make this untrue. First, the temperature scale of the instrument was calibrated for the heating stage of the thermal cycles, which involves an instrumental temperature lag in the opposite sense to that during the cooling stage; and second, during cooling, the sample lags some degrees behind the set temperature. The combination of these effects is to cause the sample temperature for $T_1 = 55°C$ not to lie sufficiently far below T_g.

The consequence of an unduly high T_1 is now discussed. On reheating, the slope of the asymptotic glassy region will be greater than it should be, and hence the peak onset temperature (T_i in *Figure 2*) will be higher than it should. This will result in the peak width being less for $T_1 = 55°C$ than it is for $T_1 = 40°C$ at the same ratio R. This effect can clearly be seen by comparing *Figures 5* and *6*, particularly at the fastest heating rates.

Effect of ratio R

The effect of the ratio R can be understood similarly. As the cooling rate (and hence R) increases, T_g occurs at higher temperatures so that at the set instrument temperature of $T_1 = 55°C$ the asymptotic glassy region is more closely approached by the sample. Higher values of R will therefore yield, for temperatures T_1 too close to T_g, lower slopes for the asymptotic glassy region. Consequently, wider peaks will result and larger corrections will need to be applied, leading to a decrease in the slope (proportional to θ^{-1}) of the plot of T_p (corr) as a function of $\log q_2$. Thus θ will increase with R and approach the true value corresponding to the use of a lower temperature T_1 (e.g. 40°C), which really does lie within the glassy region. These trends are exactly those indicated in *Table 2*.

On the other hand, for $T_1 = 40°C$, the corrected peak temperatures vary systematically with the heating rate, involving a constant value for $\theta = 0.68 \pm 0.04\ K^{-1}$.

Effect of heating rate q_2

The data in *Table 1* and *Figures 4–6* cover a range of heating rates from 2.5 to 40 K min^{-1}. The data shown in *Figure 7*, however, do not extend beyond a heating rate of 20 K min^{-1}. The reason for this restriction of the data in *Figure 7* is as follows. When the sample is reheated from the lower temperature T_1, a transient temperature gradient develops within the sample, and a certain time elapses before a steady-state temperature gradient characterized by a linear baseline (see *Figure 2*) is established. A uniform glassy condition is reached, therefore, at a temperature which increases with the heating rate q_2.

The effect of increasing heating rate in this context is shown in *Figure 3*, where it can be seen that, for a heating rate of 40 K min^{-1}, the transient regime continues to such high temperatures that a steady-state glassy region is never fully established. In fact, this transient effect was found to occur for heating rates greater than 20 K min^{-1} when the lower temperature T_1 was 40°C. If a steady-state glassy condition is never established before the onset of the peak occurs, then the theoretical analysis and the

procedure for correcting for peak width are invalidated. The same conclusion can be reached by observing the heights of the peaks in *Figure 3*. The peak height for a heating rate of 40 K min^{-1} is significantly less than that for slower heating rates, whereas the peak height should be constant for these cycles (see *Figure 1*). Accordingly, data for analysis were restricted to heating rates less than 20 K min^{-1}.

Comparison of theoretical and experimental results

Table 3 gives the theoretical temperature differences between heater and sample for various heating rates. For the fastest heating rate of 40 K min^{-1}, it can be seen that a thermal lag (between set temperature and Nth node) of the order of 2.5 K is calculated, falling rapidly to less than 0.5 K as the heating rate is reduced to 5 K min^{-1}. These results correspond well with thermal lags calculated by Richardson *et al.*[9]

With respect to the peak width, while the theoretical model shows a variation that is qualitatively in agreement with the experimental data (*Figure 10*), there are significant differences in detail. In particular: the theoretical variation reaches a limiting value below a heating rate of about 1 K min^{-1}, while the experimental data do not suggest such a limit; and the dependence on heating rate is much more marked for the theoretical model than is actually observed experimentally.

There are several possible reasons for these differences. First, the typical dependence of C_p on temperature used in these calculations (*Figure 8a*) was taken from a set of experimental data. Even though these data were obtained for a slow heating rate, they are nevertheless subject to thermal lag, and the peak in *Figure 8* is therefore wider than it would be in the absence of thermal lag. The theoretical calculations of heat transfer, however, assume *Figure 8a* to represent the real (no thermal lag) dependence of C_p on temperature. The theoretical results in *Figure 10* therefore level off at a value for the peak width which is determined by the C_p dependence shown in *Figure 8a*.

Another possibility for the differences between theory and experiment is that they could result from the simplifications inherent in the theoretical approach adopted here. In particular, the kinetics of the structural recovery behaviour, which have been treated theoretically[12] for a model system, have been separated from the heat transfer behaviour; thus the theoretical model here assumes a specific heat variation (*Figure 8*) which does not involve the kinetic aspects of structural recovery. The interaction of the theoretical kinetic and heat transfer models would be extremely complex, but it could be expected to broaden the C_p peaks (*Figure 9*), and hence flatten the theoretical curve of *Figure 10*.

CONCLUSIONS

Corrections for thermal lag in differential scanning calorimetry of polymer glasses in the glass transition region can be derived from intrinsic thermal cycles. These cycles involve cooling from equilibrium above T_g to a lower temperature T_1, and then immediately reheating to equilibrium above T_g again. It is shown that such corrections lead to a unification of the data provided that T_1 is within the asymptotic glassy region.

ACKNOWLEDGEMENTS

The authors wish to thank the SERC for funding this work.

REFERENCES

1 Volkenstein, M. V. and Sharonov, Y. A. *Vysokomol. Soed.* 1961, **3**, 1739
2 Petrie, S. E. B. *J. Polym. Sci.* (*A*-2) 1972, **10**, 1255
3 Moynihan, C. T., Easteal, A. J., Wilder, J. and Tucker, J. *J. Phys. Chem.* 1974, **78**, 2673
4 Berens, A. R. and Hodge, I. M. *Macromolecules* 1982, **15**, 756
5 Moynihan, C. T., Bruce, A. J., Gavin, D. L., Loehr, S. R. and Opalka, S. M. *Polym. Eng. Sci.* 1984, **24**, 1117
6 Stevens, G. C. and Richardson, M. J. *Polymer Commun.* 1985, **26**, 77
7 Tribone, J. J., O'Reilly, J. M. and Greener, J. *Macromolecules* 1986, **19**, 1732
8 Cowie, J. M. G. and Ferguson, R. *Polymer Commun.* 1986, **27**, 258
9 Richardson, M. J. and Burrington, P. *J. Thermal Analysis* 1974, **6**, 345
10 Richardson, M. J. *J. Polym. Sci.* (*C*) 1972, **38**, 251
11 Richardson, M. J. *Plastics Rubber Mater. Appl.* 1976, **1**, 162
12 Kovacs, A. J., Aklonis, J. J., Hutchinson, J. M. and Ramos, A. R. *J. Polym. Sci., Polym. Phys. Edn.* 1979, **17**, 1097
13 Ramos, A. R., Hutchinson, J. M. and Kovacs, A. J. *J. Polym. Sci., Polym. Phys. Edn.* 1984, **22**, 1655
14 Hutchinson, J. M. and Kovacs, A. J. *Polym. Eng. Sci.* 1984, **24**, 1087
15 Hutchinson, J. M. 'Thermal Cycling of Glasses: A Theoretical and Experimental Approach', 'Lecture Notes in Physics', Vol. 277, Springer-Verlag, Berlin, 1987, p. 172
16 Williams, G. and Watts, D. C. *Trans. Faraday Soc.* 1970, **66**, 80
17 Preston, S. D., Thomas, M. A. and Penner, G. A. 'Non-steady state performance of electrical machines', Thermodynamics and Fluid Mechanics Group, Inst. Mech. Eng., 'Heat Transfer and Fluid Flow in Electrical Machines', *Proc. Inst. Mech. Eng.* 1969–70, Vol. 184, Part 3E
18 Fried, E. 'Thermal conduction contribution to heat transfer at contacts' in 'Thermal Conductivity', Vol. 2 (Ed. R. P. Tye), Academic Press, London, 1969